Biochemistry and Biophysics Reports 37 (2024) 101605

Contents lists available at ScienceDirect

Biochemistry and Biophysics Reports

journal homepage: www.elsevier.com/locate/bbrep

Identification of prognostic risk score of disulfidptosis-related genes and molecular subtypes in glioma

Qian Jiang [1], Guo-Yuan Ling [1], Jun Yan, Ju-Yuan Tan, Ren-Bao Nong, Jian-Wen Li, Teng Deng, Li-Gen Mo [**], Qian-Rong Huang [*]

Department of Neurosurgery, Guangxi Medical University Cancer Hospital, Nanning, China

ARTICLE INFO

Keywords:
Disulfidptosis
Glioma
Prognosis
Risk score
Immunotherapy

ABSTRACT

Background: Programmed cell death is closely related to glioma. As a novel kind of cell death, the mechanism of disulfidptosis in glioma remains unclear. Therefore, it is of great importance to study the role of disulfidptosis-related genes (DRGs) in glioma.

Methods: We first investigated the genetic and transcriptional alterations of 15 DRGs. Two consensus cluster analyses were used to evaluate the association between DRGs and glioma subtypes. In addition, we constructed prognostic DRG risk scores to predict overall survival (OS) in glioma patients. Furthermore, we developed a nomogram to enhance the clinical utility of the DRG risk score. Finally, the expression levels of DRGs were verified by immunohistochemistry (IHC) staining.

Results: Most DRGs (14/15) were dysregulated in gliomas. The 15 DRGs were rarely mutated in gliomas, and only 50 of 987 samples (5.07 %) showed gene mutations. However, most of them had copy number variation (CNV) deletions or amplifications. Two distinct molecular subtypes were identified by cluster analysis, and DRG alterations were found to be related to the clinical characteristics, prognosis, and tumor immune microenvironment (TIME). The DRG risk score model based on 12 genes was developed and showed good performance in predicting OS. The nomogram confirmed that the risk score had a particularly strong influence on the prognosis of glioma. Furthermore, we discovered that low DRG scores, low tumor mutation burden, and immunosuppression were features of patients with better prognoses.

Conclusion: The DRG risk model can be used for the evaluation of clinical characteristics, prognosis prediction, and TIME estimation of glioma patients. These DRGs may be potential therapeutic targets in glioma.

1. Introduction

Originating from glial cells in the spinal cord and brain, gliomas are the most frequent primary intracranial tumors, accounting for 30 % of all central nervous system tumors [1]. Glioblastoma patients had a median overall survival (OS) time of approximately 12 months, and their OS rate for 5 years was less than 5 % [2,3]. An important factor in the low 5-year survival rate in the progression of gliomas is their invasion [4]. Men had a higher incidence of gliomas than women, and those aged 30–40 years had the highest prevalence [5]. Although glioma patients can receive various treatments, including surgical resection, chemotherapy, radiation, and electric field treatment, their prognosis is generally poor [6]. No successful targeted therapies or immunotherapies have been developed. As a result, exploring new targeted therapies and immunotherapies to improve the clinical outcomes of glioma patients is of high importance.

Recent evidence suggests that programmed cell death plays a critical role in the clearance of abnormally homeostatic cells and is considered a promising cancer treatment strategy. Depending on the mechanism, cell death is programmed in different ways, such as apoptosis, necroptosis, pyroptosis, ferroptosis, and cuproptosis. Dan Wang et al. concluded that glioma cell apoptosis could inhibit glioma cell proliferation [6]. Fang's research demonstrated the complex role of necroptosis in tumorigenesis and metastasis [7,8]. Kovacs pointed out that pyroptosis plays a major part in tumor development and therapeutic mechanisms [9]. Recently, Liu's research identified a new method of cell death that was distinct

* Corresponding author.
** Corresponding author.
E-mail addresses: ligenmo@163.com (L.-G. Mo), huangqianrong@gxmu.edu.cn (Q.-R. Huang).
[1] These authors have contributed equally to this work.

https://doi.org/10.1016/j.bbrep.2023.101605
Received 19 August 2023; Received in revised form 5 December 2023; Accepted 7 December 2023

from ferroptosis, necroptosis, and pyroptosis and named it "disulfidptosis" [10]. Excessive accumulation of disulfide bonds in disulfidptosis leads to abnormal disulfide bonds between actin skeleton proteins, triggering actin network disassembly and cell death, not only advancing the basic understanding of cell homeostasis but also providing important ideas for the treatment of cancers. Liu's study suggested that disulfidptosis induced by glucose transporter (GLUT) inhibitors might be an effective strategy to treat tumors [10]. Overall, programmed cell death-related genes are associated with malignant behaviors in a variety of tumors. At present, disulfidptosis-related genes (DRGs) have been confirmed to play an important role in the progression of various tumors [11–13]. However, there have been few studies on DRGs in glioma, and we speculate that these genes may influence the progression of glioma.

In this study, we comprehensively evaluated the expression profile of DRGs through two clusters and provided a comprehensive overview of the intraglioma immune landscape. First, two subgroups were identified from 1562 glioma patients according to the level of DRG expression. Following the identification of differentially expressed genes (DEGs) based on the two disulfidptosis subtypes, 1562 glioma patients were categorized into three gene subtypes. Additionally, we investigated the glioma tumor immune microenvironment (TIME) and developed a DRG risk score to predict prognosis and immunotherapy sensitivity.

2. Materials and methods

2.1. Datasets

Fig. 1 illustrates the flow of our research. Four glioma cohorts (TCGA, CGGA_693, CGGA_325, and GSE43378) and a normal brain tissue cohort (GTEx) were included in our research. The expression data of the TCGA (RNA-seq) were acquired from The Cancer Genome Atlas (TCGA) (https://portal.gdc.cancer. gov/), and the relevant clinicopathological data were acquired from the Chinese Glioma Genome Atlas (CGGA) (http://www.cgga.org.cn/). Other gene expression and clinicopathological data of glioma were acquired from CGGA and Gene Expression Omnibus (GEO) (https://www.ncbi.nlm.nih.gov/geo/). The RNA-seq data of normal brain samples were downloaded from GTEX (https://xenabrowser.net/datapages/). Mutation data and copy number variation (CNV) data of TCGA cohorts were acquired from the TCGA. We excluded glioma patients with indistinct World Health Organization (WHO) grades and with indistinct OS or with OS < 30 days. Therefore, 1562 glioma patients were included in the subsequent analyses. The clinical information of 1562 glioma patients is shown in Table 1. We

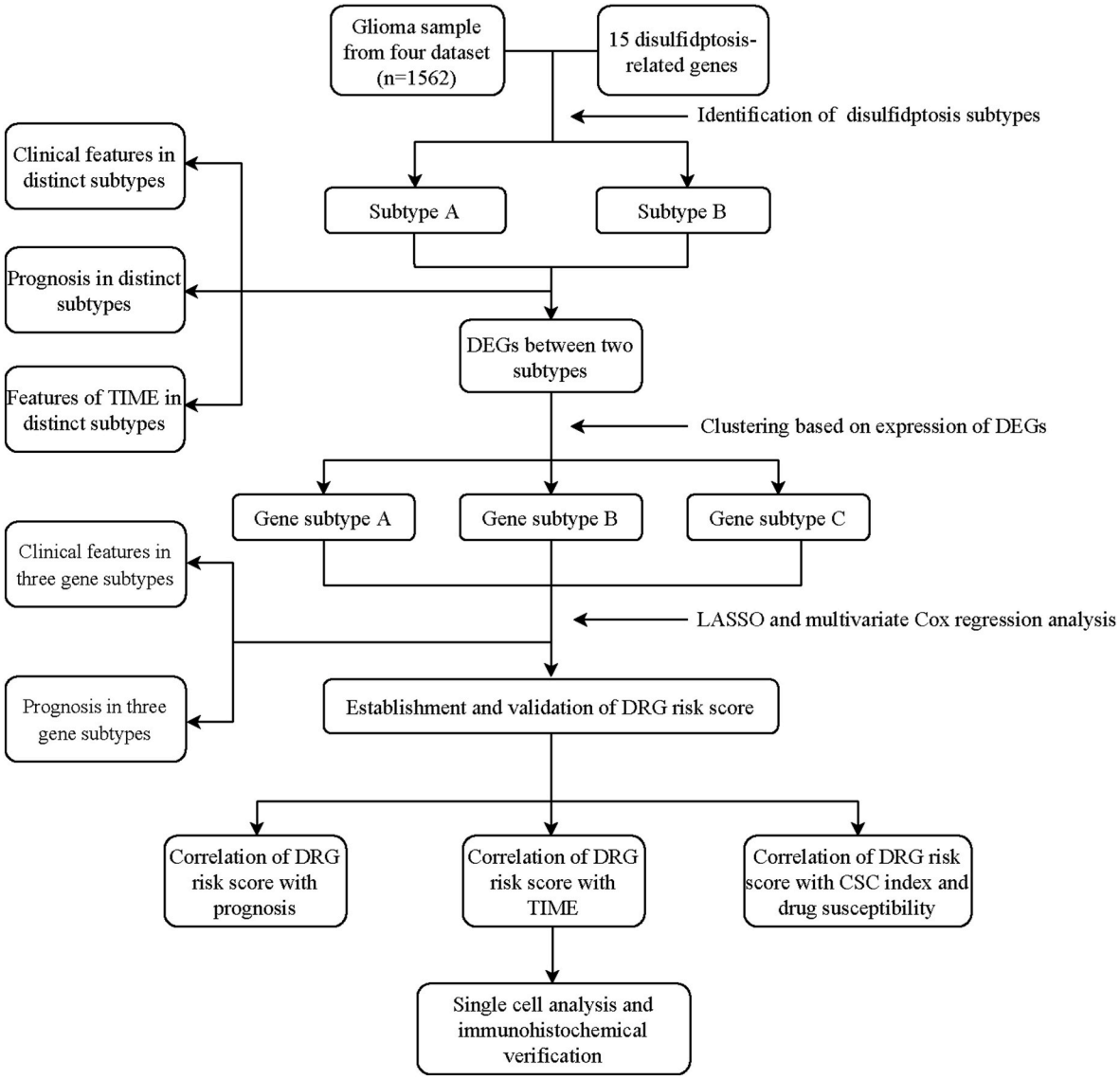

Fig. 1. The whole research process of this study.

Table 1
Clinical features of glioma patients in this study.

Clinicopathological features	TCGA	CGGA-693	CGGA-325	GEO
Age				
≤65	479	626	293	35
>65	79	29	7	14
NA	0	1	0	0
Gender				
Male	236	374	186	34
Female	321	282	114	15
WHO grade				
II	196	172	96	5
III	215	248	72	13
IV	146	236	132	31
IDH status				
Mutant	343	332	161	NA
Wild-type	208	276	139	NA
NA	6	48	0	NA
1p/19q status				
Codel	138	137	62	NA
Non-codel	414	453	238	NA
NA	5	66	0	NA
MGMT promoter status				
Methylated	NA	304	146	NA
Un-methylated	NA	217	136	NA
NA	NA	135	18	NA

TCGA: The Cancer Genome Atlas; CGGA: Chinese Glioma Genome Atlas; GEO: Gene Expression Omnibus WHO: World Health Organization; IDH: isocitrate dehydrogenase; MGMT: O-6-methylguanine-DNA methyltransferase.

used the function "remove batch effect" in the "sva" package in R software to merge RNA-sequencing of TCGA-Glioma and GTEx-Brain for differential expression analysis and combine TCGA datasets, CGGA_693 datasets, CGGA_325 datasets, and GSE43378 datasets for further analysis [14].

2.2. Expression, mutation, and CNV analyses of DRGs in glioma

Fifteen DRGs were obtained from the most current studies [10]. We downloaded glioma expression data from the UCSC Xena (https://xenabrowser.net/datapages/) website for comparison with GTEx data. We used the "remove batch effect" function in the "sva" package in R software to merge RNA sequencing of TCGA-Glioma and GTEx-Brain [14]. Then, we compared the expression of DRGs in glioma and normal brain tissue using the "limma" R package in the combined samples [15]. The mutant landscape of these 15 DRGs was shown by using the waterfall map created by the "maftools" R package [16]. In addition, we investigated the somatic CNVs in these genes.

2.3. DRGs cluster analysis

Pursuant to the expression of 15 DRGs, we divided the datasets combining TCGA, CGGA_693, CGGA_325 and GSE43378 into two clusters through the "ConsensusClusterPlus" package [17]. Clustering selection criteria: First, the sample size of each group was similar. Second, the within-group correlation was large, and the between-group correlation was small. In addition, we explored the relationship between DRG subtypes, clinical features and outcomes to determine the clinical value of the two DRG subtypes. In addition, differences in OS between the two DRG subtypes were evaluated using survival curves drawn by the "Survival" and "Survminer" packages.

2.4. Gene Ontology (GO) and Kyoto Encyclopedia of Genes and Genomes (KEGG) analysis

We identified different pathways of biological function between the two DRG subtypes using the "GSVA" R package [18]. To explore different functions between the two DRG subtypes, we applied the "limma" R package to recognize the DEGs [15]. Criteria for defining DEGs: $|\log2FC| \geq 0.585$ and adjusted p value < 0.05. The "clusterProfiler" R package was applied for GO and KEGG analysis of DEGs [19].

2.5. DEG cluster analysis

Univariate Cox regression analysis of DEGs was conducted to screen for the genes closely linked to glioma OS, which we called prognostic DEGs. Pursuant to the quantity of expression of prognostic DEGs, we divided the datasets combining TCGA, CGGA_693, CGGA_325 and GSE43378 into three clusters through the "ConsensusClusterPlus" R package [17]. We explored the relationship between DEG subtypes, clinical features and molecular markers to determine the clinical value of the three DEG subtypes. Furthermore, differences in OS between three DEG subtypes were compared using survival curves drawn by the "Survival" and "Survminer" R packages.

2.6. Establishment of the prognostic DRG risk score

The total glioma patients were randomly divided into a training group (n = 781) and a testing group (n = 781) with a proportion of approximately 1:1. In the training cohort, we included the prognostic DEGs in the LASSO analysis in R to reduce overfitting DEGs (utilizing R's "glmnet" package) [20]. Then, the signature genes and their regression coefficients were determined by multivariate Cox regression analysis. computation of risk scores for glioma patients: risk Score = Σ(Exp(i) * coef(i)), where Coef and Exp represent the coefficient and the expression level of prognostic DEGs, respectively. Adopting the median DRG risk score as the cutoff, glioma patients in the training group, testing group and all samples were divided into high-risk and low-risk groups and subjected to Kaplan–Meier (KM) survival analysis and receiver operating characteristic (ROC) curve analysis.

2.7. Establishment and validation of a prognostic nomogram

First, we removed all of the groups of glioma cases that had complete clinical data. Then, to ascertain whether the DRG risk score had independent predictive relevance, univariate/multivariate Cox regression was performed in conjunction with clinical features. In addition, based on the results of univariate/multivariate Cox regression analysis, a nomogram was created using the "RMS" package, and calibration plots and time ROC curves were used to thoroughly assess the nomogram's predictive power. The nomogram could show the contribution of each impact factor.

2.8. Characteristics of TIME cell infiltration

For every glioma patient, we assessed the stromal and immune scores using the ESTIMATE algorithm [21]. Additionally, the CIBERSORT method was used to determine the scores of 22 immune cell subpopulations for every glioma patient [22]. Then, we investigated the relationships between the DRG risk score, immune checkpoint-related genes, tumor mutation burden (TMB) and cancer stem cells (CSCs).

2.9. Single-cell RNA sequence (scRNA-seq) analysis and immunohistochemistry (IHC) verification

Tumor Immune Single Cell Hub (TISCH) can visualize single-cell transcriptome data [23]. In TISCH, we investigated the expression of 12 genes used to construct the DRG risk score at single-cell resolution. In the HPA database, we verified the expression of 10 genes used to construct the DRG risk score in glioma and normal brain tissue.

2.10. Statistical analysis

The Wilcoxon test was used for comparison in the two groups, and the Kruskal–Wallis test was used for comparison in the three groups.

Differences in OS among subgroups were assessed using the log–rank test. Spearman analysis was used to assess correlations. The remaining methods are described in detail in the Methods section. R software (v4.2.1) was applied for total statistical analyses. $P < 0.05$ was considered statistically significant.

3. Results

3.1. Differential expression analysis

As shown in Fig. 2A, 9 genes (FLNA, MYH9, TLN1, ACTB, MYH10, CAPZB, PDLIM1, CD2AP, and SLC7A11) were significantly upregulated in glioma tissues, while 5 genes (FLNB, MYL6, DSTN, IQGAP1, and INF2) were significantly upregulated in normal brain tissue.

3.2. Genetic alteration of the 15 DRGs in glioma

The waterfall plot showed the frequency of somatic mutations in these 15 DRGs, which were relatively low in the glioma cohort (Fig. 2B). Only 50 of 987 (5.07 %) samples had genetic mutations. FLNA was the most frequently mutated gene, but only two percent of the time. SLC7A11, CAPZB, MYL6, DSTN, ACTB, PDLIM1, INF2 and CD2AP did not have any mutations. In CNV analysis, the frequency of copy number gain of TLN1, FLNA and IQGAP1 was greater than the frequency of copy number loss, while the frequency of copy number loss of INF2, ACTN4, MYL6, ACTB, CAPZB, PDLIM1, CD2AP, MYH9, TLNB, SLC7A11, MYH10 and DSTN was greater than the frequency of copy number gain (Fig. 2C). In the copy number circle plot, we found the distribution of CNVs and CNVs in DRGs (Fig. 2D).

3.3. Identification of disulfidptosis-related subtypes in glioma patients

To show the characteristics of glioma patients more comprehensively, we combined the expression information of TCGA, CGGA_693, CGGA_325 and GSE43378 and underwent batch correction, which included 1562 glioma patients. Then, to investigate the value of DRGs in

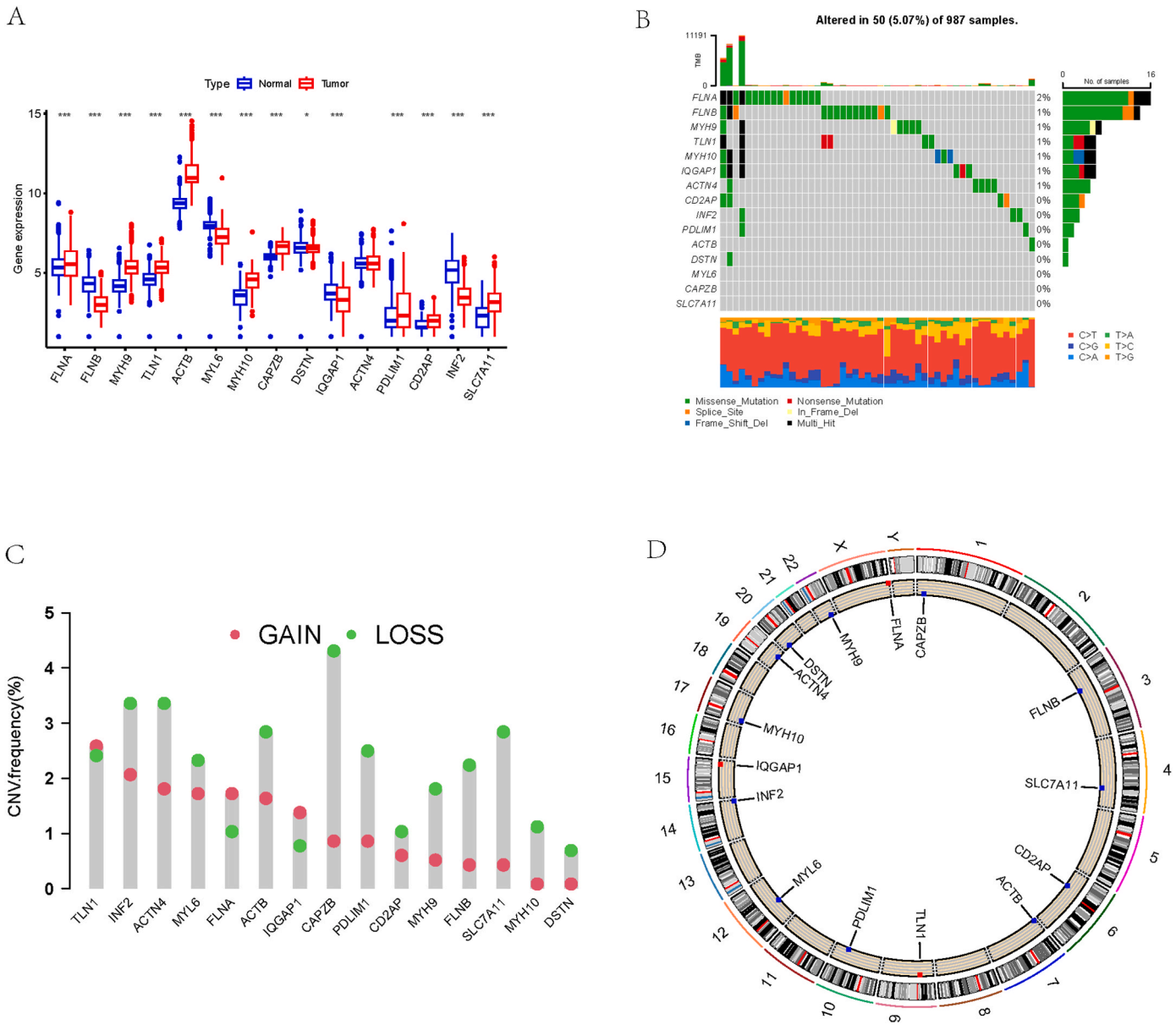

Fig. 2. Expression and genetic alteration analyses. (A) Differential expression of 15 DRGs in normal and glioma tissues. (B) Mutation frequencies of 15 DRGs in the TCGA cohort. (C) CNV of 15 DRGs. (D) CNV localization of 15 DRGs on chromosomes.

glioma prognosis, we conducted KM analysis in the combined set. The results of KM analysis manifested that all 15 genes were closely linked with the OS of glioma (Fig. 3A). Our prognostic network map suggested that CAPZB, MYL6, ACTB, TLN1, MYH9, FLNB, FLNA, CD2AP, PDLIM1, ACTN4 and IQGAP1 were the risk factors in glioma, while the DSTN, MYH10, INF2 and SLC7A11 were the favorable factors in glioma (Fig. 3B). Based on the "Consensus Cluster Plus" R package, we determined the best k value for clustering to be k = 2 (Fig. 4A). In addition, we performed principal component analysis (PCA), the results of which indicated the reliability of the clustering (Fig. 4B). We also performed survival analysis and discovered that the prognosis of glioma patients in Cluster A glioma was significantly better than that in Cluster B (Fig. 4C). We further compared the differences in DRGs expression and clinicopathological features between the two clusters. The relatively high expression of CD2AP, TLN1, MYH9, ACTN4, MYL6, PDLIM1, FLNA, IQGAQ1 and ACTB in Cluster B and MYH10 in Cluster A suggested that these DRGs might be key markers to identify different clusters (Fig. 4D). Intriguingly, we found Cluster A had a higher proportion of isocitrate dehydrogenase (IDH) mutation status, 1p19q codeletion and O-6-methylguanine-DNA methyltransferase (MGMT) methylation, which might explain the better prognosis of this cluster.

3.4. Comparison of the TIME in the two DRG subtypes

The infiltration abundances of the vast majority of immune cells in Cluster B were significantly higher than those in Cluster A, and the infiltration abundances of monocytes in Cluster A were significantly higher than those in Cluster B (Fig. 4E). Enrichment analysis of GSVA showed that subtype A was significantly enriched in immune-related and metabolism-related pathways, including antigen processing and presentation, complement and coagulation cascades, leukocyte transendothelial migration, glycosaminoglycan degradation, glycan biosynthesis, starch and sucrose metabolism, galactose metabolism, focal adhesion and the jak stat signaling pathway (Fig. 4F).

3.5. Identification of DEG subtypes in glioma patients

First, we obtained 3498 DEGs through differential analysis of the two DRG subtypes. Then, univariate Cox regression analysis was conducted to identify the 3498 differentially expressed genes, and 3497 prognostic DEGs were identified. To further explore the regulatory mechanism of disulfidptosis, we used a consensus clustering algorithm to classify glioma patients into three subtypes on the basis of the expression of prognostic DEGs, including Cluster A, Cluster B, and Cluster C (Fig. 5A). Survival analysis was conducted, and the results suggested that the prognosis of glioma patients in Cluster A was the best and Cluster B was the worst (Fig. 5B). In addition, the three DEG subtypes showed significant differences in DRG expression (Fig. 5C). Interestingly, we found that Cluster A had the highest percentage of 1p19q codeletions, which might explain why this cluster had the best prognosis (Fig. 5D). GO enrichment analysis showed that DEGs were enriched in cell signal transduction-related biological processes (Fig. 5E). KEGG analysis showed that DEGs were enriched in cancer-related pathways, indicating that DEGs played an important role in glioma progression (Fig. 5F).

3.6. Development and validation of a DRG risk score

We established a DRG risk score in the training group. Computation of risk scores for glioma patients = (0.164638375191975 * expression of NFE2L3) - (expression of ARL3 * 0.249060961628408) - (0.159952892626383*expression of AMZ1) + (0.161263746815120 expression of PBX) + (0.0902646983989976 * expression of HOXD9) - (0.208875684755589 * expression of MKX) - (0.232461723016582 * expression of FXYD2) - (0.121331890778999 * expression of SAMD11) + (0.304541275576046 * expression of FSCN1)- (0.17006620014416 * expression of CLVS1)- (0.223160069617897 * expression of SEMA3G) + (0.172302760245823 * expression of TP73). Glioma patients in the training group were segmented into high-risk and low-risk groups by using the median risk score as the cut-off. Then, we validated the risk score in the testing group, which was also segmented into high- and low-risk groups on the basis of the median value of the DRG risk score in the training group. Fig. 6A shows the differential expression of 15 DRGs between the two groups. Through the risk distribution map of the DRG cluster, we found that the DRG risk score of Cluster B was significantly higher than that of Cluster A, which was consistent with our previous study showing that the prognosis of glioma patients in Cluster A was significantly better than that in Cluster B (Fig. 6B). The risk distribution map of the DEG cluster indicated that the DRG risk scores of Cluster A, Cluster B and Cluster C were significantly different (Fig. 6C). This finding was based on the results of our previous three prognostic DRG survival analyses. Fig. 6D shows the process of constructing a DRG risk score. In addition, survival analyses were performed in two DRG risk groups. The KM curve of the training group, testing group and all samples showed that the OS of the low-risk group was significantly longer than that of the high-risk group with higher AUC values (Fig. 7A-O).

3.7. Construction of a nomogram

We identified grade, 1p19q codeletion status and DRG risk score as independent prognostic factors for glioma prognosis using univariate and multivariate Cox regression analyses (Fig. 8A and B). The nomogram showed the contribution of each influencing factor, and risk score, tumor grade and 1p19q codeletion status were the factors that significantly affected the prognosis (Fig. 8C). Calibration curves at 1, 3, and 5 years were also generated, which indicated the high predictive accuracy of the nomogram (Fig. 8D). ROC curves were used to predict the sensitivity and specificity of 1-, 3-, and 5-year survival of the nomogram and AUC values were 0.829, 0.882, and 0.880, respectively (Fig. 8E–H).

3.8. Comparison of the TIME between the two risk groups

We explored the associations of 22 immune cells with risk scores and 12 genes were used to construct the model. The immune-related heatmap suggested that the DRG risk score was positively related to native B cells, macrophages, neutrophils, CD8 T cells, follicular helper T cells and regulatory T cells and negatively related to memory B cells, resting dendritic cells, eosinophils, activated mast cells, monocytes, activated NK cells and resting memory CD4 T cells. We also found that the 12 genes were associated with almost all immune cells (Fig. 9A and B). In addition, we explored the correlation between DRGs and immune checkpoints and found that the majority of immune checkpoints were significantly increased in the high-risk group (Fig. 9C). Furthermore, the stromal score, immune score and ESTIMATE score were used to quantify the tumor microenvironment. Interestingly, the high-risk score was positively related to the stromal score, immune score, and ESTIMATE score (Fig. 9D).

3.9. Mutation and Csc index analysis

Previous research has demonstrated that since individuals with high TMB have more neoantigens, they may benefit more from immunotherapy [24]. When we compared TMB in the high- and low-risk groups, we discovered that the DRG risk score and TMB were positively correlated, suggesting that the high-risk group may benefit from immunotherapy (Fig. 10A and B). The variations in the somatic mutation distribution between the two DRG risk groups were next examined. IDH1, TP53, and ATRX were the top 3 mutated genes in both the high- and low-risk groups (Fig. 10C and D). To evaluate glioma stem cell characteristics, we also performed a stem cell association analysis and found an inverse relationship between the DRG risk score and the Csc index. Scatter plots of stem cell association indicated that the high-risk

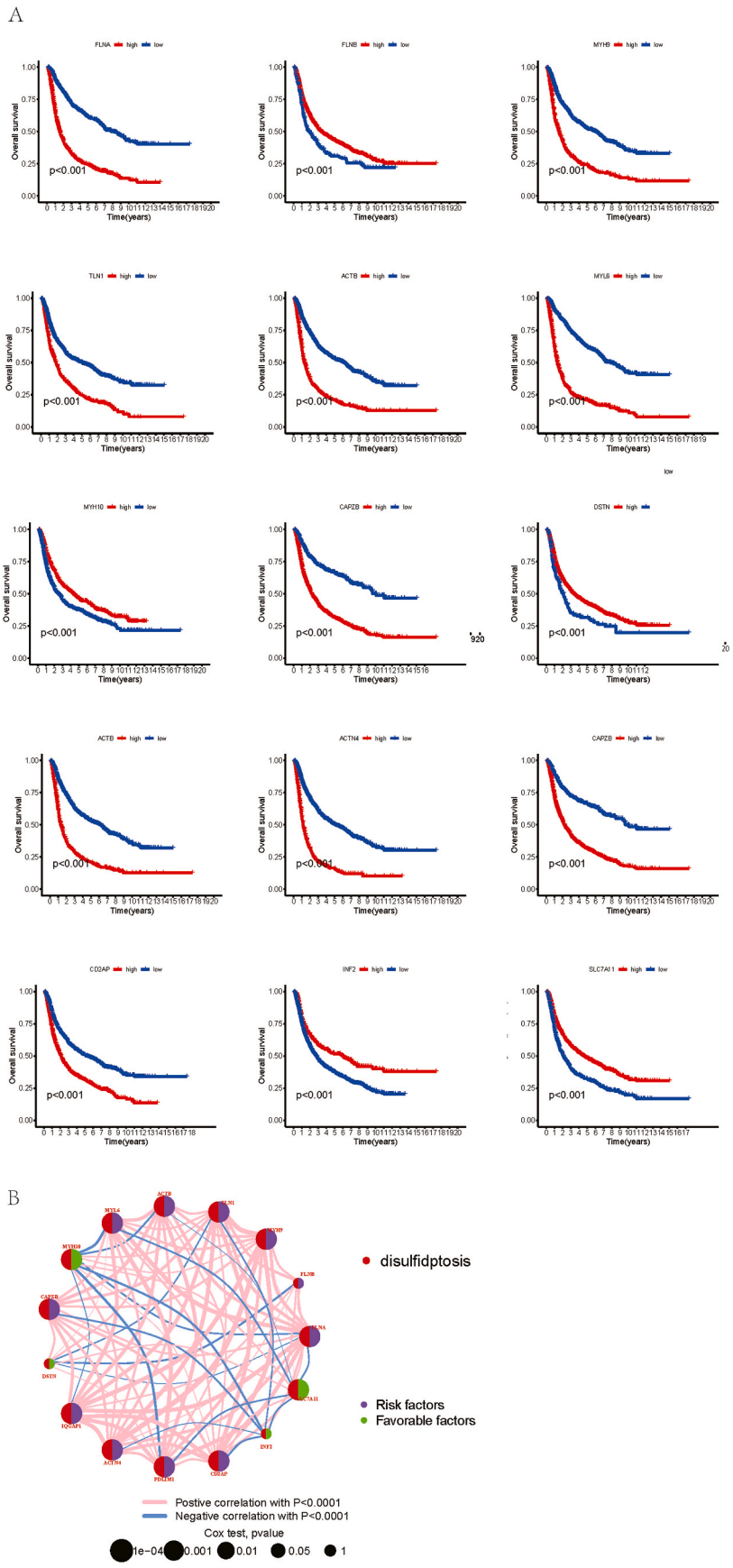

Fig. 3. Identification of prognostic DRGs and the relationship between DRGs. (A) All 15 DRGs were glioma prognostic-related genes. (B) The right half of the circle in green represents the protective genes, while the right half of the circle in purple represents the risk genes. The two DRGs connected by the pink line are positively correlated, while the two DRGs connected by the blue line are negatively correlated.

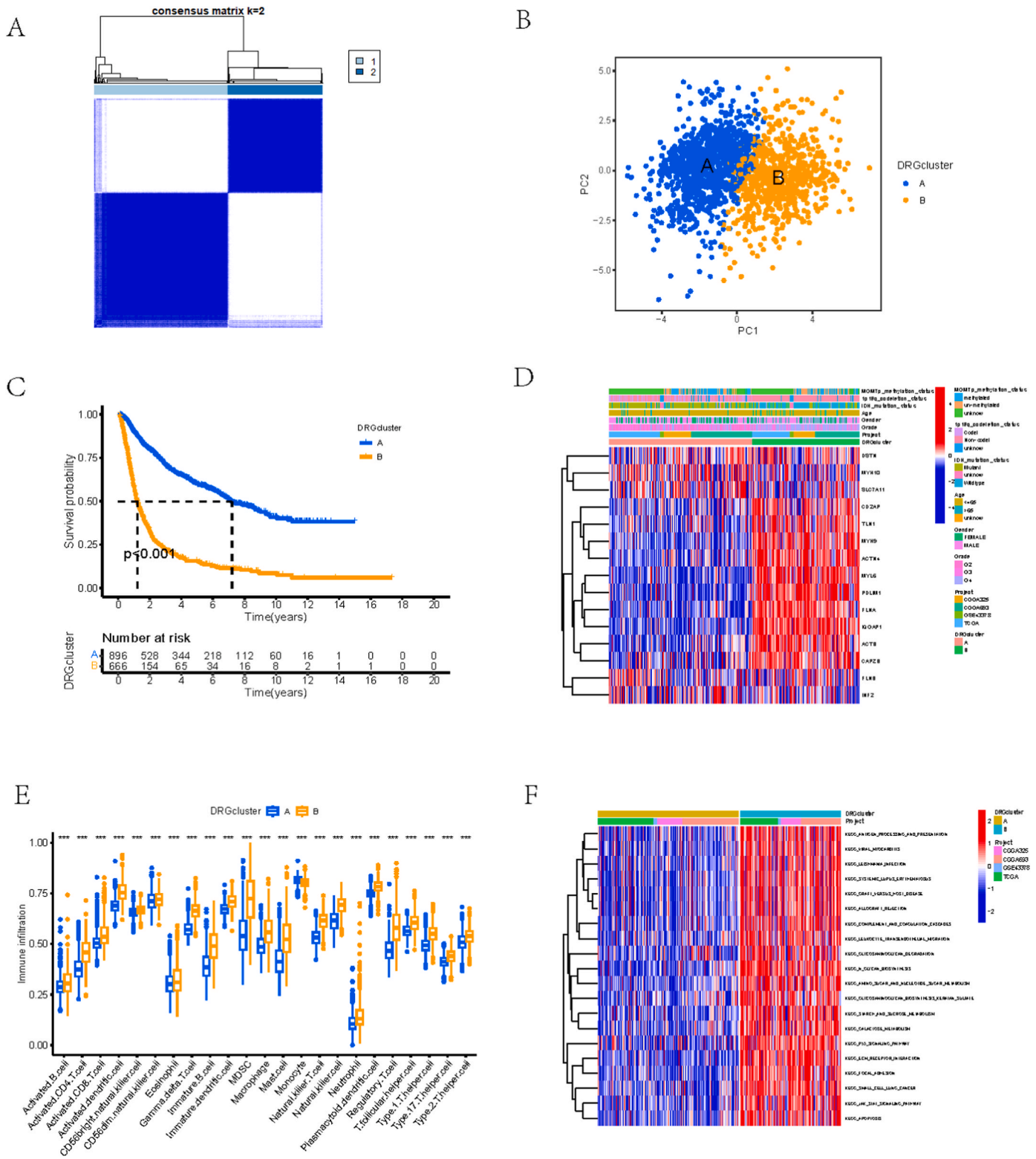

Fig. 4. Identification of DRG clusters and correlation between DRG clusters, clinical features, TIME, and prognosis. (A) Heatmap depicting consensus clustering solution (k = 2). (B) Principal component analysis plots. (C) Kaplan-Meier curves of DRG cluster A and DRG cluster B. (D) Clinical features of DRG cluster A and DRG cluster B. (E) Abundance of 22 infiltrating immune cell types of DRG cluster A and DRG cluster B. (F) GSVA analysis for DRG cluster A and DRG cluster B.

group had a lower Csc index and a higher degree of cell differentiation (Fig. 10E).

3.10. Validation of DRG expression patterns via scRNA-seq analysis and the HPA database

To confirm the detailed cell types expressing these 12 genes that were used to construct DRG risk scores, we analyzed single-cell data

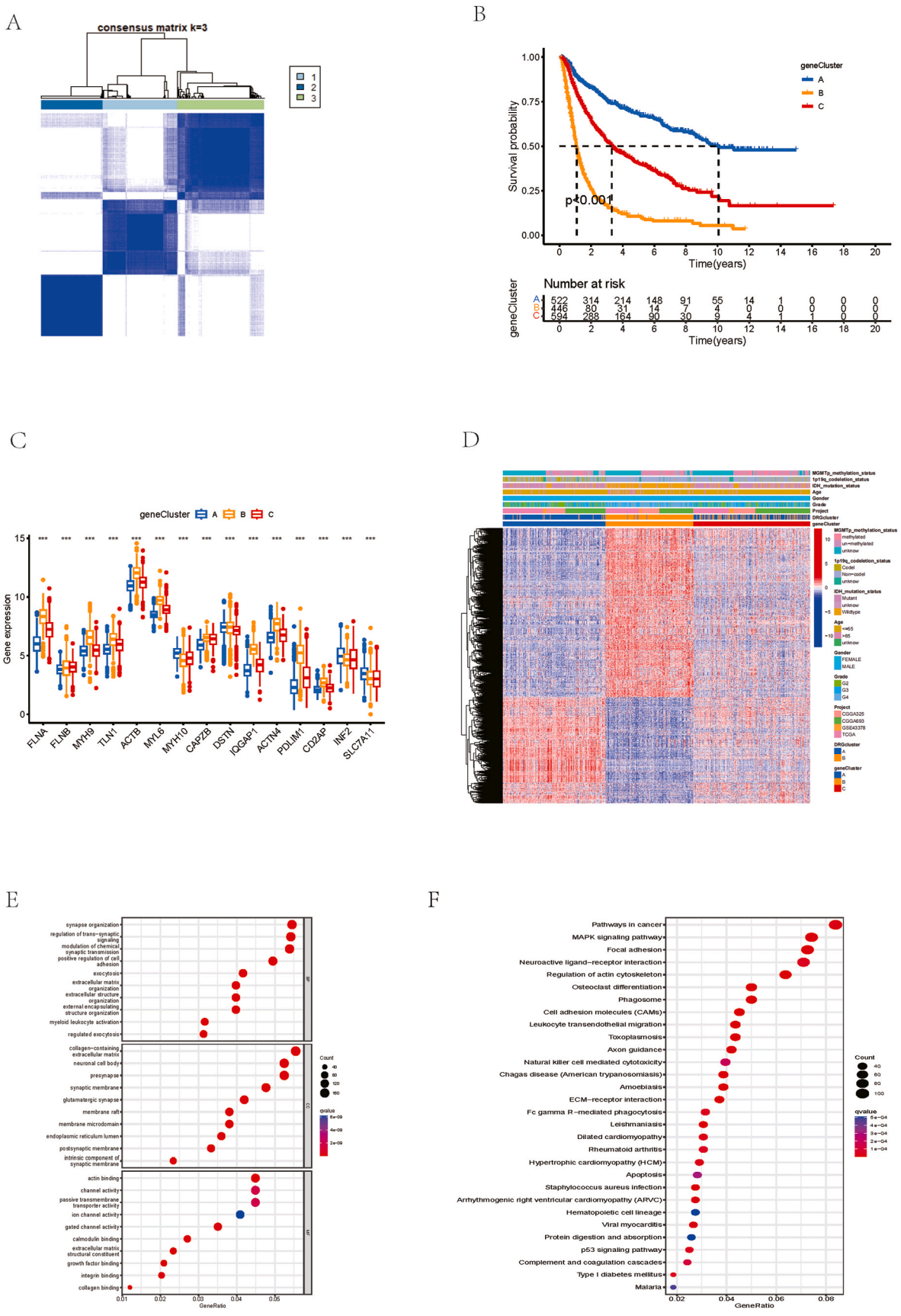

Fig. 5. Identification of DEG clusters and correlation between DEG clusters, clinical features, and prognosis. (A) Heatmap depicting consensus clustering solution (k = 3). (B) Kaplan-Meier curves of gene cluster A, gene cluster B, and gene cluster C. (C) Distribution of DRGs expression in the three gene clusters. (D) Clinical features of the three gene clusters (E) GO enrichment analysis of DEGs. (F) KEGG enrichment analysis of DEGs.

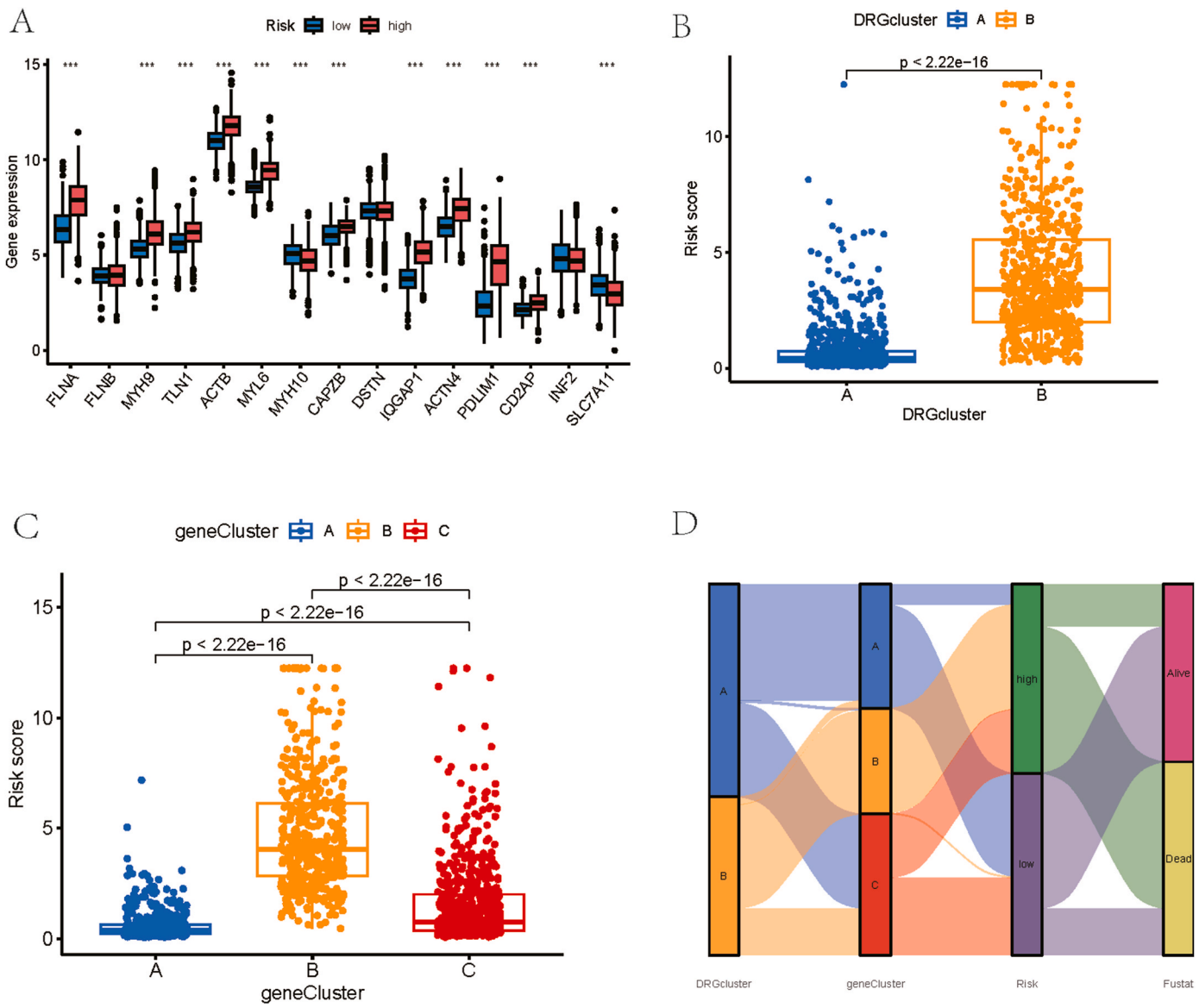

Fig. 6. Construction and grouping of DRG risk score. (A) Differential expression of 15 DRGs between high- and low-risk groups. (B) Differences in risk scores between DRG cluster A and DRG cluster B. (C) Differences in risk scores between three gene clusters. (D) Alluvial plot of the process of constructing a prognostic model.

from GSE148842. We detected six cell clusters, including AC-like malignant, CD8Tex, malignant, mono/macro, oligodendrocyte and others by single-cell analysis (Fig. 11A). We found that ARL3 and FSCN1 were highly expressed in malignant cells (Fig. 11B and C). In addition, most of the genes were expressed at low levels in Mono/macro and CD8Tex cells. There were no immunohistochemical data for HOXD9 and SAMD11 in the HPA database. We compared the IHC for 10 genes that were used to construct DRG risk scores in different WHO stages based on the HPA database (Fig. 12). ARL3 was moderately expressed in normal brain tissue but expressed at low levels in gliomas. AMZ1 was highly expressed in normal brain tissues but not in gliomas. PBX3 was expressed at low levels in normal brain tissues but was moderately expressed in gliomas. MKX was highly expressed in normal brain tissues but moderately expressed in gliomas. FSCN1 was moderately expressed in normal brain tissues and low-grade gliomas but highly expressed in high-grade gliomas. CLVS1 and SEMA3G were moderately expressed in normal brain tissues but not expressed in gliomas. There was no significant difference in the expression of NFE2L3, FXYD2, and TP73 in normal brain tissues, low-grade glioma, and high-grade glioma.

4. Discussion

Previous studies have shown that programmed cell death-related genes play a major role in predicting the prognosis and treatment of glioma [25–27]. The role of disulfidptosis in glioma inception and progression remains unclear. Furthermore, immunotherapy has shown remarkable results in treating tumors such as liver and lung cancer, but it had no discernible effect on the overall survival of glioma patients. Therefore, we explored the value of DRGs in gliomas and the potential of DRGs as targets for glioma immunotherapy. Based on the expression of DRGs, we clustered all glioma samples into two subtypes and found significant differences in clinical features, prognostic features and TIME between the two subtypes. Then, on the basis of the expression of DEGs in the two DRG subtypes, we clustered all glioma samples into three subtypes and found significant differences in clinical features and prognosis among the three subtypes. The results of the two rounds of clustering indicated that DRGs could be used as a potential target for immunotherapy and in evaluating the prognosis of gliomas. Moreover, we constructed a 12-gene DRG prognostic risk score and evaluated its predictive power. There were significant differences in prognosis, TMB,

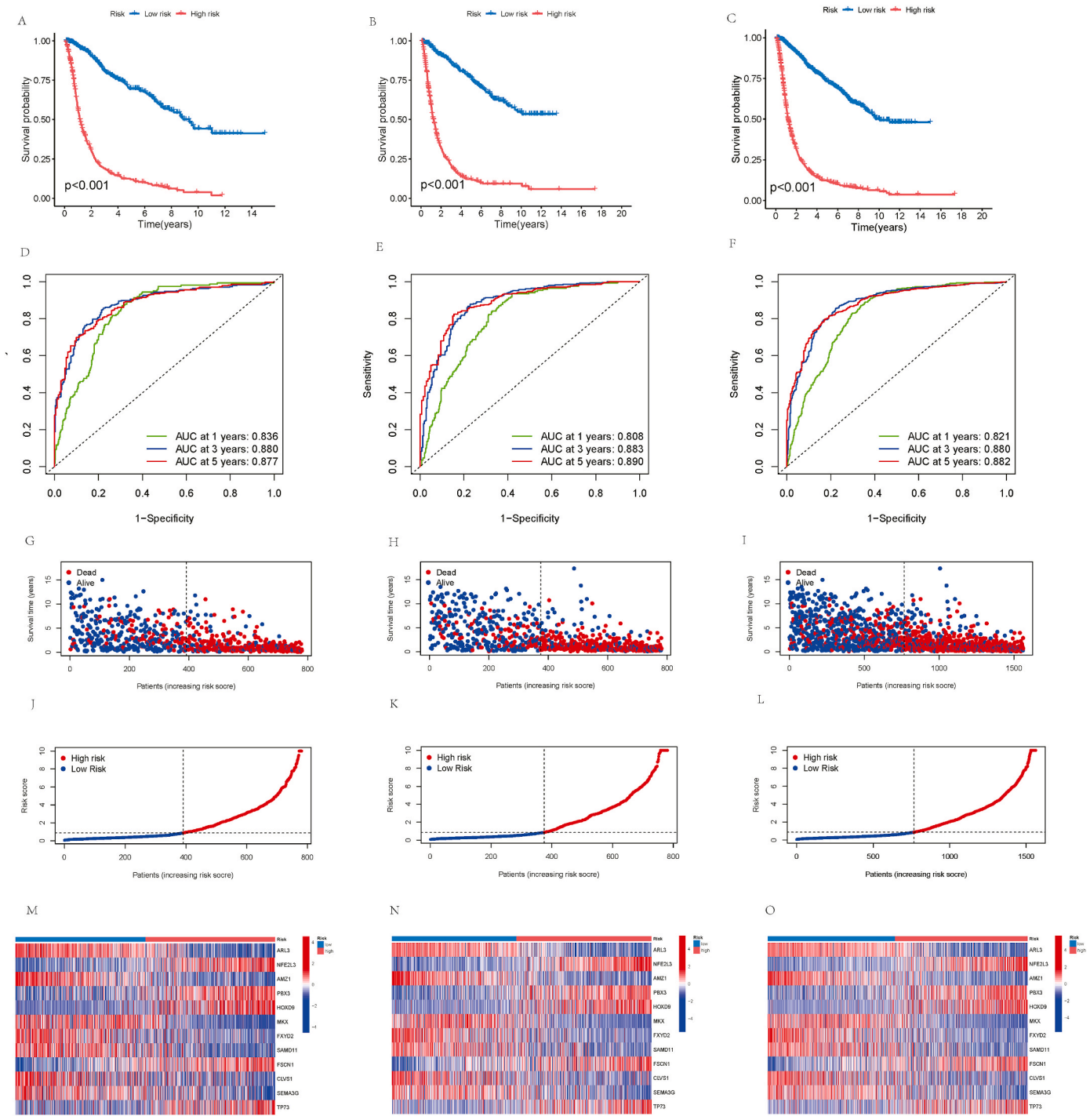

Fig. 7. Validation of the DRG risk score. (A) Kaplan-Meier curves of high and low-risk groups in the training group. (B) Kaplan-Meier curves of high and low-risk groups in the testing group. (C) Kaplan-Meier curves of high and low-risk groups in all samples. (D–F) ROC curves to predict the sensitivity and specificity of 1-, 3-, and 5-year survival according to the DRG risk score in the training group, testing group, and all samples. (G–L) distribution plot of risk score and survival status in the training group, testing group, and all samples. (M – O) A risk heatmap of 12 genes used to construct the risk score in the training group, testing group, and all samples.

TIME and CSC index between the two risk groups. The results showed that the high-risk group with poor prognosis had a higher immune score, which was contrary to the lower immune score in a high-risk group of colorectal cancer risk models in the past, but this partly explained the lack of survival benefit of immunotherapy in the treatment of glioblastoma [28]. Finally, we developed a nomogram to predict the OS of glioma patients and verified that it had good predictive power, which assisted in making clinical decisions. Previously, Wang et al. constructed a DRG signature in glioma and showed good predictive ability. Our DRG signature includes more genes, which can more comprehensively display the biological characteristics of glioma. Moreover, the AUC values of our DRG signature in the testing group (0.808, 0.883, and 0.890 at 1, 3, and 5 years, respectively) were higher than theirs (0.620, 0.750, and 0.710 at 1, 3, and 5 years, respectively), showing more accurate prediction performance [29]. In addition, compared to another recent study on DRGs, our DRG signature is suitable for both low-grade

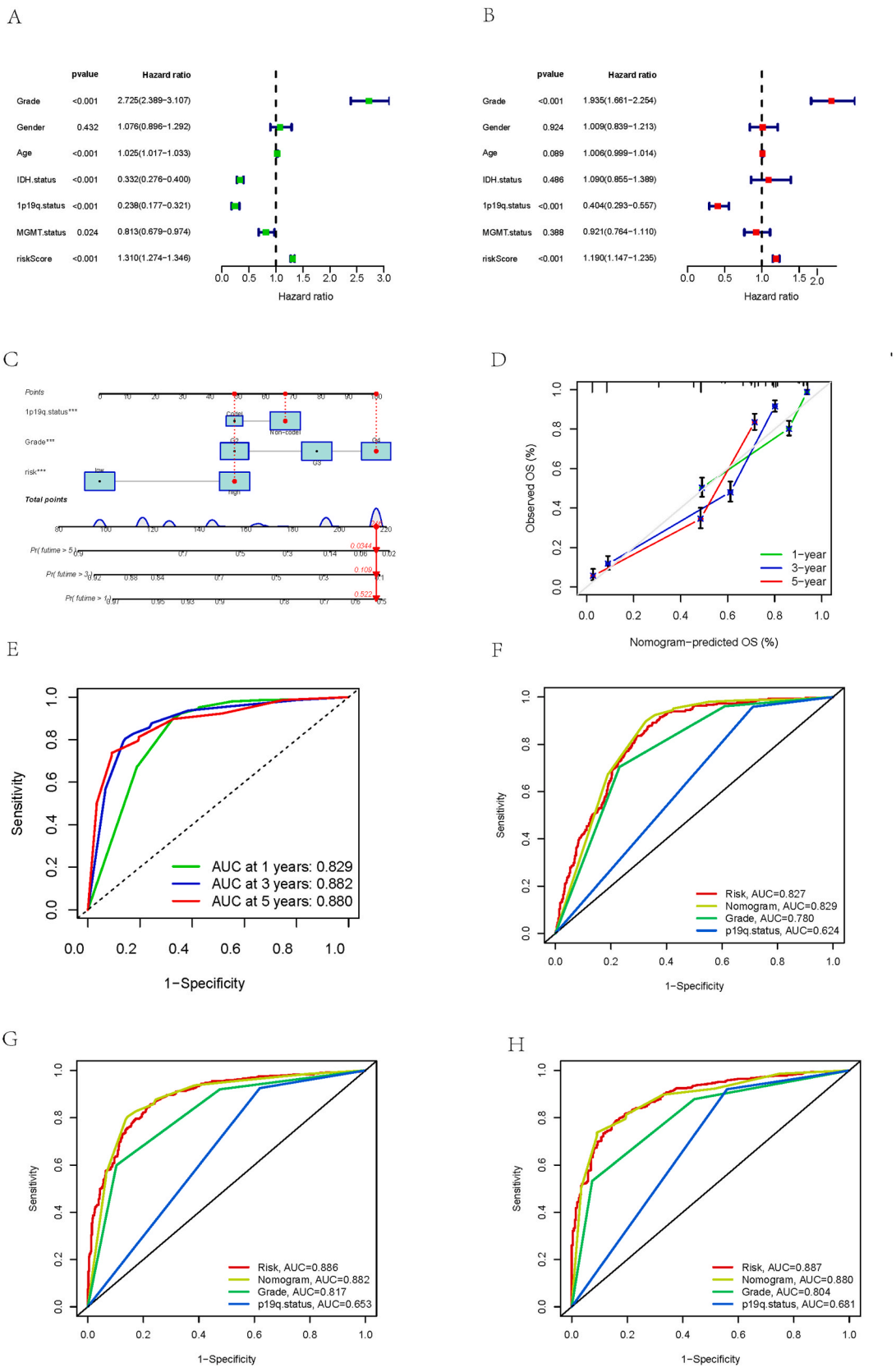

Fig. 8. Construction and validation of a nomogram. (A–B) Univariate and multivariate Cox regression analysis. (C) Nomogram for predicting 1-, 3-, and 5-year survival. (D)The calibration plot for nomogram. (E–H) ROC curves to predict the sensitivity and specificity of 1-, 3-, and 5-year survival of the nomogram and independent prognostic factors.

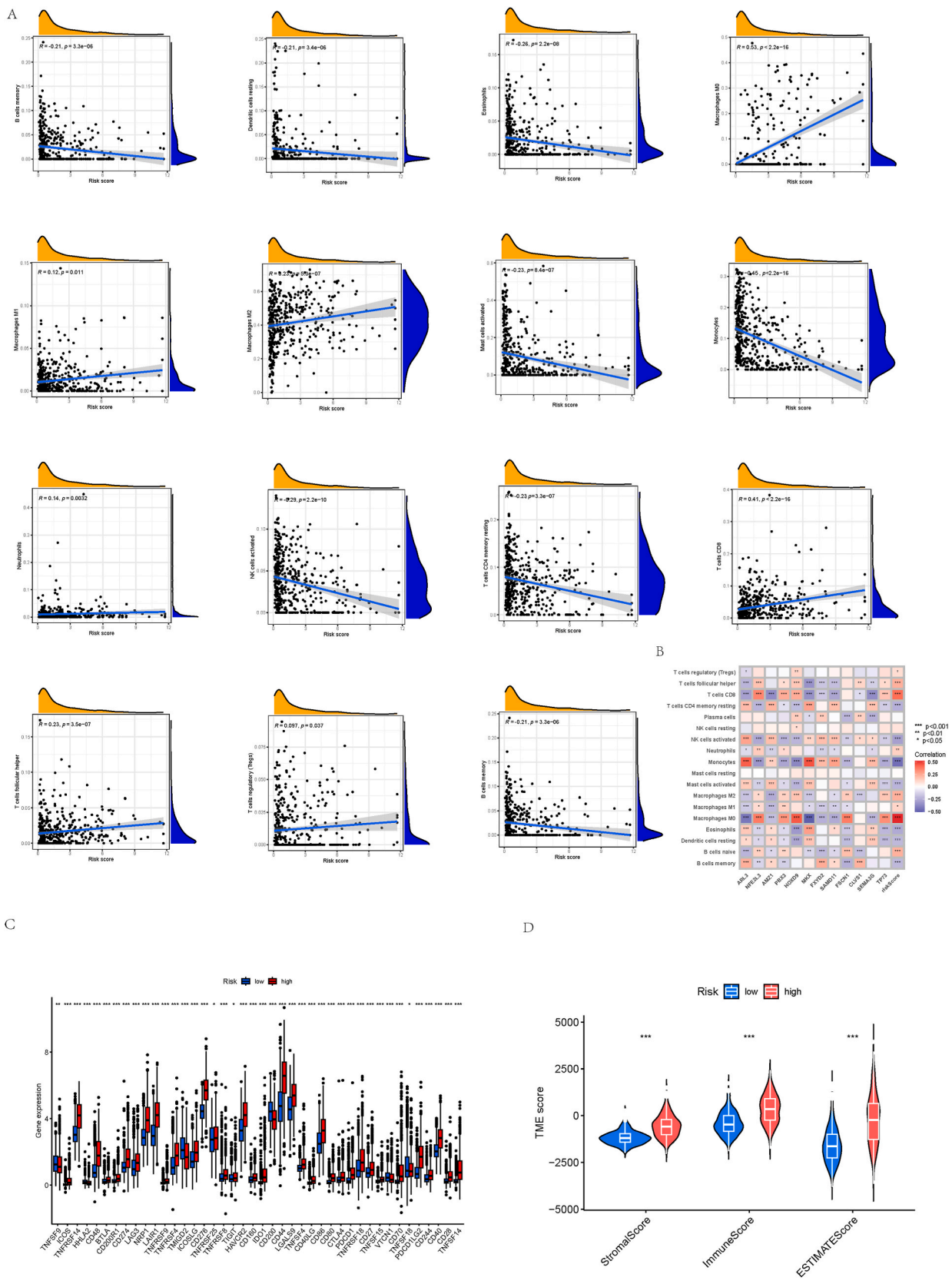

Fig. 9. Correlation between DRGs and TIME. (A) Correlation of immune cells and 12 genes used to construct DRG risk score. (B) Correlation of immune cells and DRG risk score. (C)Differential expression of immune checkpoint-related genes in high- and low-risk groups. (D) Differences in immune-related scores between the high and low-risk groups.

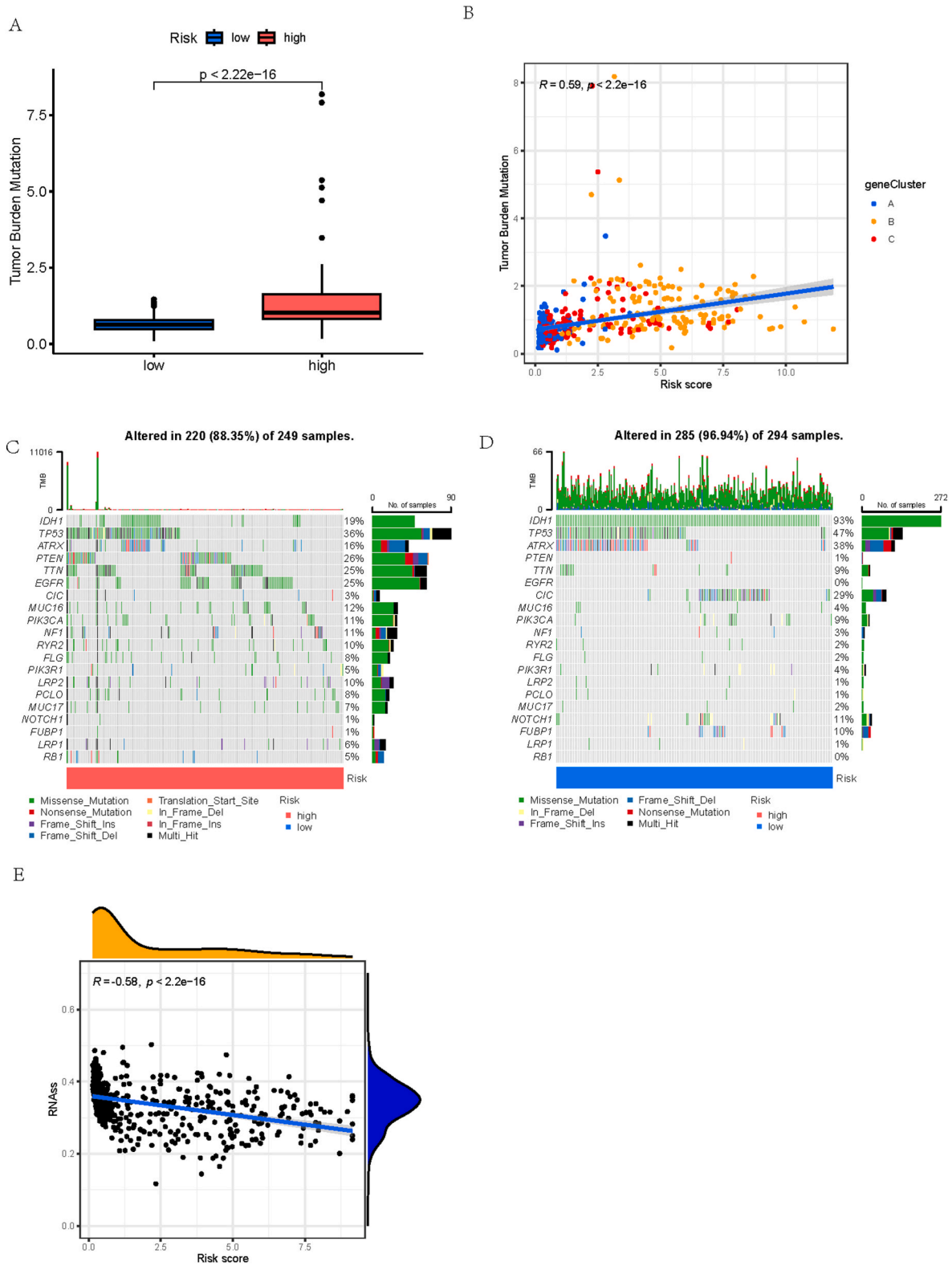

Fig. 10. Correlation between DRG risk score, Csc index, and TMB. (A–D) Correlation between TMB and DRG risk scores. (E) Correlation between Csc index and DRG risk scores.

and high-grade gliomas [30]. Therefore, this study is a good complement to glioma survival prediction methods.

The molecular functions of these 12 genes were analyzed to explore their roles in the genesis and progression of glioma. As a protective factor, ARL3 is a glioma prognostic marker and therapeutic target that participates in immune cell infiltration in the GBM immune microenvironment [31]. ARL3 affects the outcomes of glioma by regulating the immune microenvironment [31]. NFE2L3 was not only trapped in the regulation of the cell cycle but was also related to apoptosis, differentiation and inflammation of tumor cells, indicating that it might

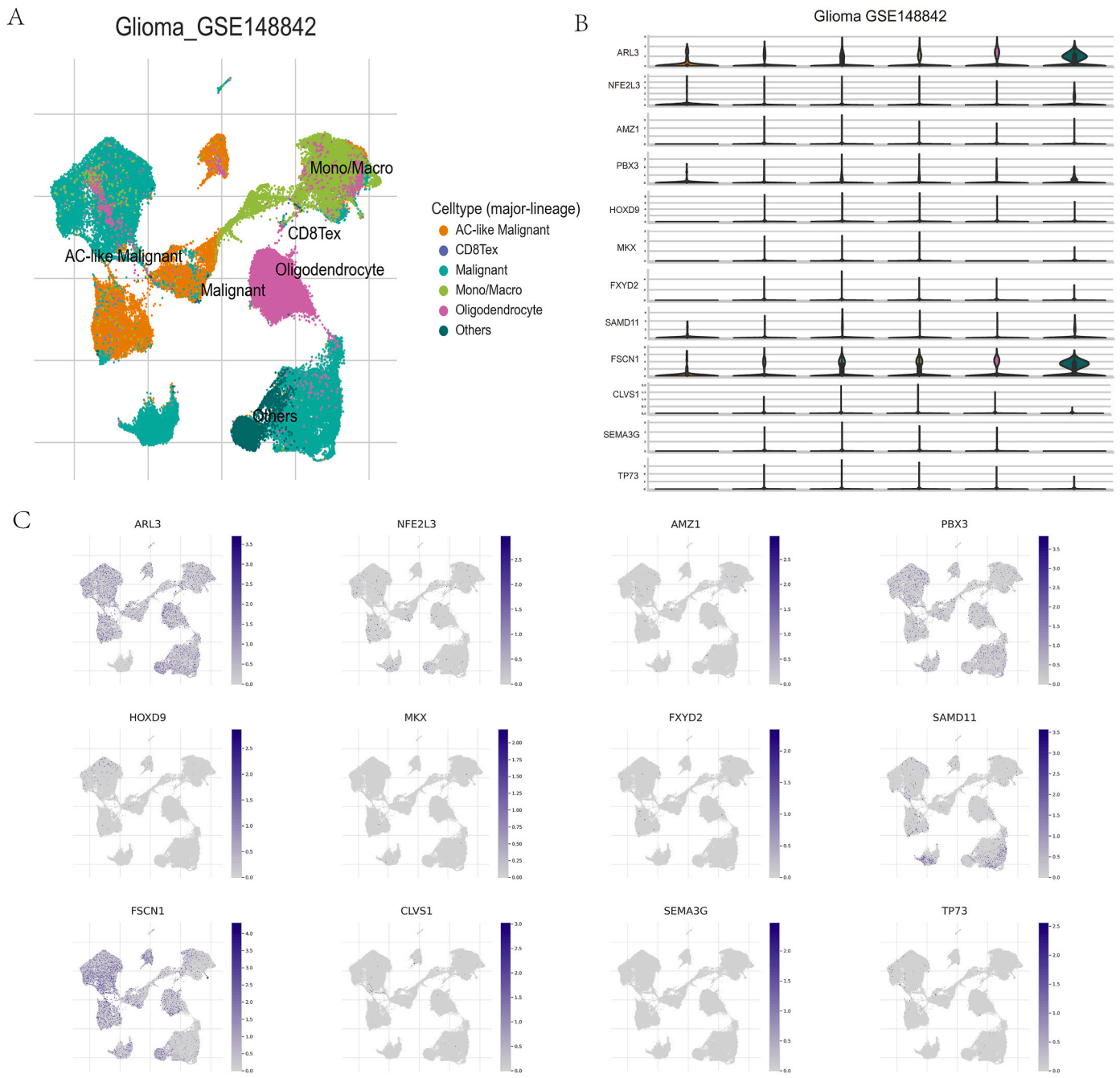

Fig. 11. Analysis of Single-cell data in GSE148842. (A) Cell composition in the GSE148842 database. (B–C) Expression of the 12 genes used to construct DRG risk scores in each cell in GSE148842.

participate in disulfidptosis-related processes [32]. In addition, NFE2L3 could protect against colorectal cancer by modulating the tumor microenvironment, indicating its potential as a prognostic predictor for glioma [33]. PBX3 is a marker of many kinds of tumors [34]. As a risk factor, PBX3 increased the metastasis and invasion of glioblastoma, which was consistent with our study [35]. HOXD9 is a proliferation marker of glioma stem cells [36]. As the γ subunit of Na/K-ATPase, FXYD2 is a regulator of enzymatic activity [37]. FXYD2 inhibits tumor cell proliferation and survival by inhibiting the activation and expression of Na/K-ATPase, so FXYD2 can predict OS and chemotherapy sensitivity to TMZ in glioma patients [37]. FSCN1 is a highly conserved actin-binding protein. Past research has illustrated that FSCN1 is highly expressed in many cancers and that its overexpression is usually associated with tumor spread and poor outcomes [38–41]. Huang's study found that FSCN1 altered the TIME by regulating the mutual effect between tumor cells and macrophages to promote tumor development [42]. Therefore, FSCN1 is a potential target for glioma immunotherapy. Class 3 semaphorins (SEMA3) are a group of secreted glycoproteins involved in the development of the nervous system and axon guidance. As a member of the SEMA3 family of proteins, SEMA3G is highly correlated with the invasion and migration of glioma cells [43]. Edward's study showed that TP73 could regulate various aspects of programmed cell death, including cell cycle arrest and apoptosis [44]. Candi's research suggested that TP73 was associated with cancer progression and metastasis [45]. In our study, TP73 was a risk factor in the DRG risk score, which was consistent with Candi's study. AMZ1, MKX, SAMD11 and CLVS1 have only been reported in a few studies, so their relationship with glioma is not clear at present. In our study, AMZ1,

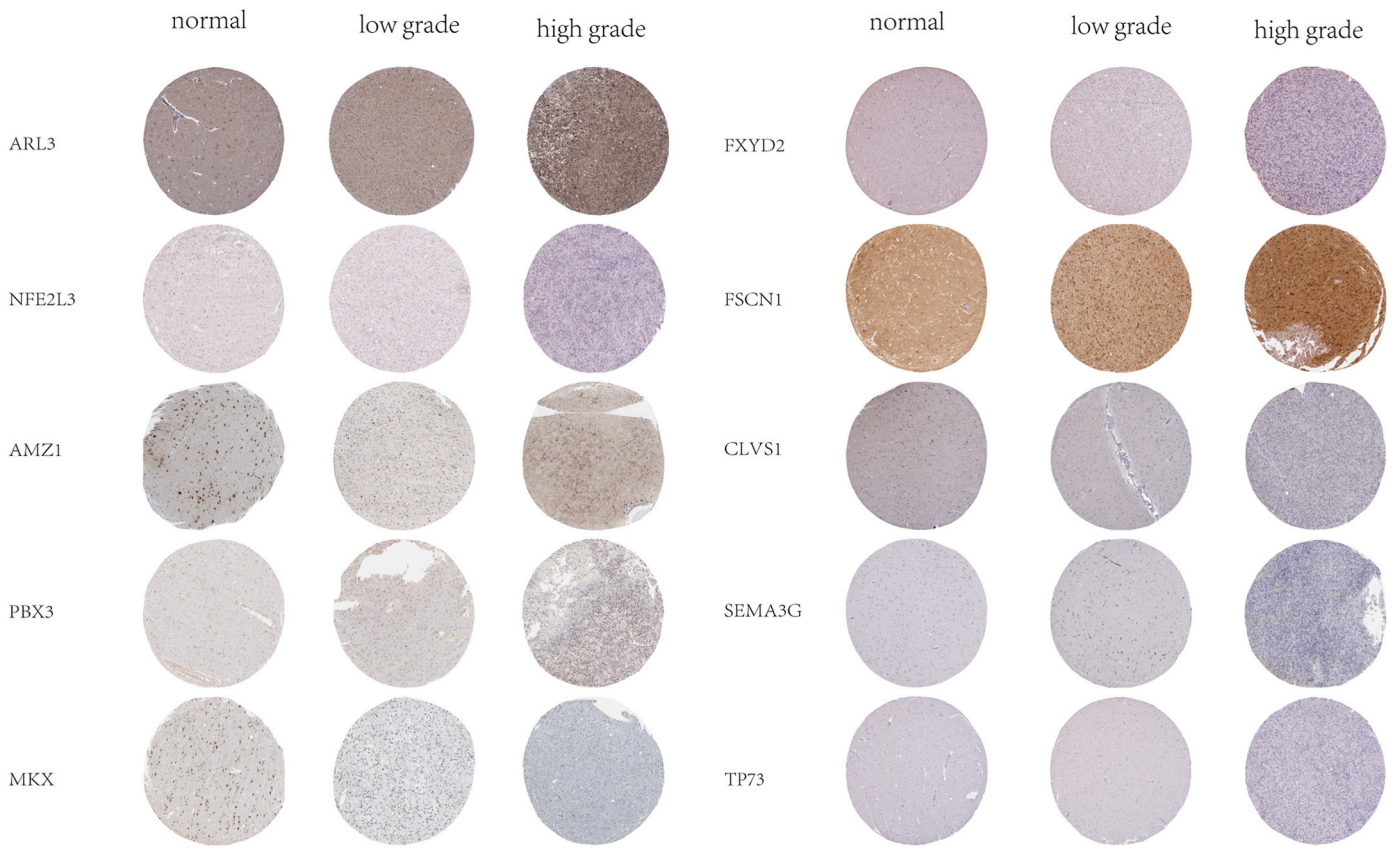

Fig. 12. IHC for 10 key genes used to construct DRG risk scores with different WHO stages.

MKX, SAMD11 and CLVS1 were identified as protective factors for glioma.

In the past decade, immunotherapy has been increasingly used in solid tumors [45]. However, there still has not been a breakthrough in the treatment of glioma. The reason might be that the features of the TIME of glioma patients were not fully recognized. The TIME of glioma is very complex, including not only many highly heterogeneous tumor cells but also various immune cells [46]. Given this, we explored the features of the TIME of glioma subtypes. In our research, subtype A was related to a lower DRG score and exhibited immune inhibition, while subtype B was related to a higher DRG risk score and exhibited immune activation. We discovered significant differences in immune cell content between subtype A and subtype B and significant differences in immune score between the two DRG risk score groups, indicating that DRGs play an important role in the origin and development of glioma. PAKAWAT's research suggested that gliomas could trigger gene mutations in T cells that cause them to lose function and return to the bone marrow, leading to the gradual collapse of the body's immune cycle [47]. Liu's study showed that the immune inhibition factors expressed by gliomas could malfunction T cells, so the large number of dysfunctional T cells in gliomas could lead to the failure of immunotherapy [48]. These studies might partly explain our finding that subtype B and the high DRG risk group had worse outcomes despite having higher T-cell infiltration. Schmidt's study showed that B cells could act as antigen-presenting cells (APCs) and interact with $CD4^+$ and $CD8^+$ T cells to improve patient outcomes in breast cancer and non-small cell lung cancer [49,50]. However, Nelson's research showed that B cells suppressed immune responses in lymphoma, colon cancer, melanoma and skin cancer [51]. According to the studies mentioned above, B lymphocytes function differently in various types of tumors. In our study, activated B cells and immature B cells in subtype B were significantly higher than those in subtype A. We also found that B-cell memory was negatively correlated with the DRG risk score, while native B cells were positively correlated with the DRG risk score. Therefore, the role of B cells in the glioma immune microenvironment needs to be further investigated. Kim's study showed that one of the greatest obstacles to the treatment of glioblastoma was the large number of immunosuppressive macrophages that accumulated in the tumor, which promoted tumor progression by mediating the expression of growth factors, enzymes and cytokines related to tumor growth and immunosuppression [52]. In this study, the number of macrophages was high in the subtype B and high-risk DRG score groups, indicating immunosuppression and insensitivity to immunotherapy in the subtype B and high-risk score groups. Currently, targeting macrophages has good application prospects in the treatment of glioma [53,54]. We found that DRG risk scores were associated with macrophage infiltration, suggesting that DRGs may be a target for targeting macrophages in glioma therapy. Clinical studies at the Andrew Cancer Research Center found that glioblastoma stem cells could inhibit natural killer (NK) cell activity by releasing TFG-β signaling proteins. However, deletion of TFG-β receptors in NK cells restored their antitumor activity [55]. Experiments at Nara Medical University in Japan found that injecting NK cells into mice with glioblastoma significantly increased the OS of the mice [56]. In our study, NK cells were higher in the subtype A and low-risk DRG score groups, indicating that glioma patients in the subtype A and low-risk DRG score groups had a better prognosis. In addition, exploring the relationship between DRGs and NK cells might be one of the ways to activate the antitumor activity of NK cells. Immunotherapy plays an increasingly important role in the comprehensive treatment of cancer. However, immune checkpoint inhibitors targeting PD-1 and CTLA 4 have not shown a significant effect in glioma clinical trials [56]. Our research indicates a strong correlation between DRGs and the glioma TIME, indicating a promising future for DRG multitarget therapy in conjunction with immune checkpoint inhibitors [57,58].

Of course, our study also has some limitations. First, the prognostic role of the DRG risk score should be validated by clinical data. Moreover, the underlying biological features related to the DRG risk score require future confirmation experiments.

5. Conclusion

The DRG risk score based on disulfidptosis molecular subtypes can be used for the evaluation of clinical characteristics, prognosis prediction, and immune microenvironment estimation of glioma patients.

Funding

This research was supported by the Youth Program of the Scientific Research Foundation of Guangxi Medical University Cancer Hospital (YQJ2022-10) and the Opening Project of Guangxi Medical and Health Appropriate Technology Development and Promotion Project (No. S2020097).

Availability of data and materials

All data generated or analyzed during the present study are included in this published article or are available from the corresponding author on reasonable request.

Ethics approval

Not applicable.

CRediT authorship contribution statement

Qian Jiang: Data curation, Software, Validation, Writing – original draft. **Guo-Yuan Ling:** Data curation, Validation, Writing – original draft. **Jun Yan:** Formal analysis, Investigation, Supervision. **Ju-Yuan Tan:** Data curation, Investigation, Resources. **Ren-Bao Nong:** Data curation, Resources, Supervision. **Jian-Wen Li:** Investigation, Project administration, Visualization. **Teng Deng:** Project administration, Resources. **Li-Gen Mo:** Conceptualization, Methodology, Project administration, Writing – review & editing. **Qian-Rong Huang:** Conceptualization, Funding acquisition, Methodology, Project administration, Resources, Writing – review & editing.

Declaration of competing interest

The authors declare that the research was conducted in the absence of any commercial or financial relationships that could be construed as a potential conflict of interest.

Data availability

Data will be made available on request.

Acknowledgements

Not applicable.

Appendix A. Supplementary data

Supplementary data to this article can be found online at https://doi.org/10.1016/j.bbrep.2023.101605.

References

[1] J. Lou, Y. Hao, K. Lin, Y. Lyu, M. Chen, H. Wang, D. Zou, X. Jiang, R. Wang, D. Jin, et al., Circular RNA CDR1as disrupts the p53/MDM2 complex to inhibit Gliomagenesis, Mol. Cancer 19 (1) (2020) 138.

[2] J. Chang, C. Kim, B. Choi, Y. Kim, J. Kim, IJJoKNS. Kim, Pseudoprogression and pseudoresponse in the management of high-grade glioma : optimal decision timing according to the response assessment of the neuro-oncology working group, J Korean Neurosurg 55 (1) (2014) 5–11.

[3] M. Khan, A. Sharma, M. Pitz, S. Loewen, H. Quon, A. Poulin, Essig MJCo, High-grade glioma management and response assessment-recent advances and current challenges, Curr. Oncol. 23 (4) (2016) e383–e391.

[4] C. Liang, L. Yang, SJOl Guo, All-trans retinoic acid inhibits migration, invasion and proliferation, and promotes apoptosis in glioma cells, Oncol. Lett. 9 (6) (2015) 2833–2838.

[5] H. Alexander, C. Irwin, G. Purdie, Hunn MJJocnojotNSoA, Incidence and management of high grade glioma in Māori and non-Māori patients, J. Clin. Neurosci. 17 (9) (2010) 1144–1147.

[6] Z. Xiang, Q. Lv, X. Chen, X. Zhu, S. Liu, D. Li, XJBr Peng, Lnc GNG12-AS1 knockdown suppresses glioma progression through the AKT/GSK-3β/β-catenin pathway, Biosci. Rep. 40 (8) (2020).

[7] J. Yu, S. Li, J. Qi, Z. Chen, Y. Wu, J. Guo, K. Wang, X. Sun, JJCd Zheng, disease: cleavage of GSDME by caspase-3 determines lobaplatin-induced pyroptosis in colon cancer cells, Cell Death Dis. 10 (3) (2019) 193.

[8] Y. Fang, S. Tian, Y. Pan, W. Li, Q. Wang, Y. Tang, T. Yu, X. Wu, Y. Shi, P. Ma, et al., Pyroptosis: a new frontier in cancer, Biomed. Pharmacother. 121 (2020), 109595.

[9] S. Kovacs, Miao EJTicb, Gasdermins: effectors of pyroptosis, Trends Cell Biol. 27 (9) (2017) 673–684.

[10] X. Liu, L. Nie, Y. Zhang, Y. Yan, C. Wang, M. Colic, K. Olszewski, A. Horbath, X. Chen, G. Lei, et al., Actin cytoskeleton vulnerability to disulfide stress mediates disulfidptosis, Nat. Cell Biol. 25 (3) (2023) 404–414.

[11] T. Wang, K. Guo, D. Zhang, H. Wang, J. Yin, H. Cui, WJIi Wu, Disulfidptosis classification of hepatocellular carcinoma reveals correlation with clinical prognosis and immune profile, Int. Immunopharm. 120 (2023), 110368.

[12] S. Zhao, L. Wang, W. Ding, B. Ye, C. Cheng, J. Shao, J. Liu, HJFie Zhou, Crosstalk of disulfidptosis-related subtypes, establishment of a prognostic signature and immune infiltration characteristics in bladder cancer based on a machine learning survival framework, Front. Endocrinol. 14 (2023), 1180404.

[13] C. Qi, J. Ma, J. Sun, X. Wu, J.J.A. Ding, The role of molecular subtypes and immune infiltration characteristics based on disulfidptosis-associated genes in lung adenocarcinoma, Aging (Albany NY) 15 (11) (2023) 5075–5095.

[14] J. Leek, W. Johnson, H. Parker, A. Jaffe, J.J.B. Storey, The sva package for removing batch effects and other unwanted variation in high-throughput experiments, Bioinformatics 28 (6) (2012) 882–883.

[15] M. Ritchie, B. Phipson, D. Wu, Y. Hu, C. Law, W. Shi, GJNar Smyth, Limma powers differential expression analyses for RNA-sequencing and microarray studies, Nucleic Acids Res. 43 (7) (2015) e47.

[16] A. Mayakonda, D. Lin, Y. Assenov, C. Plass, HJGr Koeffler, Maftools: efficient and comprehensive analysis of somatic variants in cancer, Genome Res. 28 (11) (2018) 1747–1756.

[17] M. Wilkerson, D.J.B. Hayes, ConsensusClusterPlus: a class discovery tool with confidence assessments and item tracking, Bioinformatics 26 (12) (2010) 1572–1573.

[18] S. Hänzelmann, R. Castelo, Guinney JJBb, GSVA: gene set variation analysis for microarray and RNA-seq data, BMC Bioinf. 14 (2013) 7.

[19] G. Yu, L. Wang, Y. Han, Q.J. He, Oajoib: clusterProfiler: an R package for comparing biological themes among gene clusters, OMICS 16 (5) (2012) 284–287.

[20] S. Engebretsen, JJCe Bohlin, Statistical predictions with glmnet, Clin. Epigenet. 11 (1) (2019) 123.

[21] Z. Ke, Y. Wu, P. Huang, J. Hou, Y. Chen, R. Dong, F. Lin, Y. Wei, X. Xue, C. Ng, et al., Identification of novel genes in testicular cancer microenvironment based on ESTIMATE algorithm-derived immune scores, J. Cell. Physiol. 236 (1) (2021) 706–713.

[22] B. Chen, M. Khodadoust, C. Liu, A. Newman, AJMimb Alizadeh, Profiling tumor infiltrating immune cells with CIBERSORT, Methods Mol. Biol. 1711 (2018) 243–259.

[23] D. Sun, J. Wang, Y. Han, X. Dong, J. Ge, R. Zheng, X. Shi, B. Wang, Z. Li, P. Ren, et al., TISCH: a comprehensive web resource enabling interactive single-cell transcriptome visualization of tumor microenvironment, Nucleic Acids Res. 49 (2021) D1420–D1430.

[24] A. Snyder, V. Makarov, T. Merghoub, J. Yuan, J. Zaretsky, A. Desrichard, L. Walsh, M. Postow, P. Wong, T. Ho, et al., Genetic basis for clinical response to CTLA-4 blockade in melanoma, N. Engl. J. Med. 371 (23) (2014) 2189–2199.

[25] W. Shao, Z. Yang, Y. Fu, L. Zheng, F. Liu, L. Chai, JJFic Jia, Biology d: the pyroptosis-related signature predicts prognosis and indicates immune microenvironment infiltration in gastric cancer, Front. Cell Dev. Biol. 9 (2021), 676485.

[26] B. Chao, F. Jiang, H. Bai, P. Meng, L. Wang, FJJoc Wang, m medicine, Predicting the prognosis of glioma by pyroptosis-related signature, J. Cell Mol. Med. 26 (1) (2022) 133–143.

[27] H. Zhang, Z. Wang, Z. Dai, W. Wu, H. Cao, S. Li, N. Zhang, QJFii Cheng, Novel immune infiltrating cell signature based on cell pair algorithm is a prognostic marker in cancer, Front. Immunol. 12 (2021), 694490.

[28] W. Song, J. Ren, R. Xiang, C. Kong, T.J.O. Fu, Identification of pyroptosis-related subtypes, the development of a prognosis model, and characterization of tumor microenvironment infiltration in colorectal cancer, OncoImmunology 10 (1) (2021), 1987636.

[29] X. Wang, J. Yang, F. Yang, KJSr Mu, The disulfidptosis-related signature predicts prognosis and immune features in glioma patients, Sci. Rep. 13 (1) (2023), 17988.

[30] X. Li, S. Liu, D. Liu, Y. Li, X. Cai, Y. Su, ZJOm Xie, Identification of disulfidptosis-related genes and immune infiltration in lower-grade glioma, Open Med. 18 (1) (2023), 20230825.
[31] Y. Wang, W. Zhao, X. Liu, G. Guan, MJJotm Zhuang, ARL3 is downregulated and acts as a prognostic biomarker in glioma, J. Transl. Med. 17 (1) (2019) 210.
[32] M. Liu, H. Wei, J. Yang, X. Chen, H. Wang, Y. Zheng, Y. Wang, YJFig Zhou, Multi-omics analysis of molecular characteristics and carcinogenic effect of NFE2L3 in pan-cancer, Front. Genet. 13 (2022), 916973.
[33] J. Saliba, B. Coutaud, K. Makhani, N. Epstein Roth, J. Jackson, J. Park, N. Gagnon, P. Costa, T. Jeyakumar, M. Bury, et al., Loss of NFE2L3 protects against inflammation-induced colorectal cancer through modulation of the tumor microenvironment, Oncogene 41 (11) (2022) 1563–1575.
[34] H. Han, Y. Du, W. Zhao, S. Li, D. Chen, J. Zhang, J. Liu, Z. Suo, X. Bian, B. Xing, et al., PBX3 is targeted by multiple miRNAs and is essential for liver tumour-initiating cells, Nat. Commun. 6 (2015) 8271.
[35] X. Xu, Z. Bao, Y. Liu, K. Jiang, T. Zhi, D. Wang, L. Fan, N. Liu, JJJoe Ji, CR ccr: PBX3/MEK/ERK1/2/LIN28/let-7b positive feedback loop enhances mesenchymal phenotype to promote glioblastoma migration and invasion, J. Exp. Clin. Cancer Res. 37 (1) (2018) 158.
[36] M. Tabuse, S. Ohta, Y. Ohashi, R. Fukaya, A. Misawa, K. Yoshida, T. Kawase, H. Saya, C. Thirant, H. Chneiweiss, et al., Functional analysis of HOXD9 in human gliomas and glioma cancer stem cells, Mol. Cancer 10 (2011) 60.
[37] N. Minor, Q. Sha, C. Nichols, RJPotNAoSotUSoA. Mercer, The gamma subunit of the Na,K-ATPase induces cation channel activity, Proc Natl Acad 95 (11) (1998) 6521–6525.
[38] J. Liang, Z. Liu, X. Wei, L. Zhou, Y. Tang, C. Zhou, K. Wu, F. Zhang, F. Zhang, Y. Lu, et al., Expression of FSCN1 and FOXM1 are associated with poor prognosis of adrenocortical carcinoma patients, BMC Cancer 19 (1) (2019) 1165.
[39] M. Kano, N. Seki, N. Kikkawa, L. Fujimura, I. Hoshino, Y. Akutsu, T. Chiyomaru, H. Enokida, M. Nakagawa, Matsubara HJIjoc, miR-145, miR-133a and miR-133b: tumor-suppressive miRNAs target FSCN1 in esophageal squamous cell carcinoma, Int. J. Cancer 127 (12) (2010) 2804–2814.
[40] I. Gupta, S. Vranic, H. Al-Thawadi, A.J.C. Al Moustafa, Fascin in gynecological cancers: an update of the literature, Cancers 13 (22) (2021).
[41] C. Wang, C. Tang, Y. Wang, L. Jin, Q. Wang, X. Li, G. Hu, B. Huang, Y. Zhao, CJSr Su, FSCN1 gene polymorphisms: biomarkers for the development and progression of breast cancer, Sci. Rep. 7 (1) (2017), 15887.
[42] Y. Huang, G. Shan, Y. Yi, J. Liang, Z. Hu, G. Bi, Z. Chen, J. Xi, D. Ge, Q. Wang, et al., FSCN1 induced PTPRF-dependent tumor microenvironment inflammatory reprogramming promotes lung adenocarcinoma progression via regulating macrophagic glycolysis, Cell. Oncol. 45 (6) (2022) 1383–1399.
[43] X. Zhou, L. Ma, J. Li, J. Gu, Q. Shi, RJOr Yu, Effects of SEMA3G on migration and invasion of glioma cells, Oncol. Rep. 28 (1) (2012) 269–275.
[44] Ratovitski EJA-caimc: dehydroleucodine induces a TP73-dependent transcriptional regulation of multiple cell death target genes in human glioblastoma cells, Anti Cancer Agents Med. Chem. 17 (6) (2017) 839–850.
[45] E. Candi, M. Agostini, G. Melino, FJHm Bernassola, How the TP53 family proteins TP63 and TP73 contribute to tumorigenesis: regulators and effectors, Hum. Mutat. 35 (6) (2014) 702–714.
[46] X. Wang, H. Cao, Y. Zhai, S. Deng, M. Chao, Y. Hu, Y. Mou, S. Guo, W. Zhao, C. Li, et al., Immune gene signatures and immunotypes in immune microenvironment are associated with glioma prognose, Front. Immunol. 13 (2022), 823910.
[47] P. Chongsathidkiet, C. Jackson, S. Koyama, F. Loebel, X. Cui, S. Farber, K. Woroniecka, A. Elsamadicy, C. Dechant, H. Kemeny, et al., Sequestration of T cells in bone marrow in the setting of glioblastoma and other intracranial tumors, Nat. Med. 24 (9) (2018) 1459–1468.
[48] S. Liu, X. Liu, C. Zhang, W. Shan, XJFip Qiu, T-cell exhaustion status under high and low levels of hypoxia-inducible factor 1α expression in glioma, Front. Pharmacol. 12 (2021), 711772.
[49] M. Schmidt, D. Böhm, C. von Törne, E. Steiner, A. Puhl, H. Pilch, H. Lehr, J. Hengstler, H. Kölbl, Gehrmann MJCr, The humoral immune system has a key prognostic impact in node-negative breast cancer, Cancer Res. 68 (13) (2008) 5405–5413.
[50] K. Al-Shibli, T. Donnem, S. Al-Saad, M. Persson, R. Bremnes, LJCcraojotAAfCR. Busund, Prognostic effect of epithelial and stromal lymphocyte infiltration in non-small cell lung cancer 14 (16) (2008) 5220–5227.
[51] BJJoi Nelson, CD20+ B cells: the other tumor-infiltrating lymphocytes, J. Immunol. 185 (9) (2010) 4977–4982.
[52] H. Kim, J. Park, H. Kim, C. Kim, I. Kang, HJNc Lee, Blood monocyte-derived CD169 macrophages contribute to antitumor immunity against glioblastoma, Nat. Commun. 13 (1) (2022) 6211.
[53] W. Zhou, S. Ke, Z. Huang, W. Flavahan, X. Fang, J. Paul, L. Wu, A. Sloan, R. McLendon, X. Li, et al., Periostin secreted by glioblastoma stem cells recruits M2 tumour-associated macrophages and promotes malignant growth, Nat. Cell Biol. 17 (2) (2015) 170–182.
[54] C. Poon, S. Sarkar, V. Yong, JJBajon Kelly, Glioblastoma-associated microglia and macrophages: targets for therapies to improve prognosis, Brain 140 (6) (2017) 1548–1560.
[55] H. Shaim, M. Shanley, R. Basar, M. Daher, J. Gumin, D. Zamler, N. Uprety, F. Wang, Y. Huang, K. Gabrusiewicz, et al., Targeting the αv integrin/TGF-β axis improves natural killer cell function against glioblastoma stem cells, J. Clin. Invest. (14) (2021) 131.
[56] J. Fares, Z. Davis, J. Rechberger, S. Toll, J. Schwartz, D. Daniels, J. Miller, Khatua SJNpo, Advances in NK cell therapy for brain tumors, npj Precis. Oncol. 7 (1) (2023) 17.
[57] Z. Wang, Y. Liu, Y. Mo, H. Zhang, Z. Dai, X. Zhang, W. Ye, H. Cao, Z. Liu, QJFii Cheng, The CXCL family contributes to immunosuppressive microenvironment in gliomas and assists in gliomas chemotherapy, Front. Immunol. 12 (2021), 731751.
[58] X. Liang, Z. Wang, Z. Dai, H. Zhang, Q. Cheng, ZJJoo Liu, Promoting prognostic model application: a review based on gliomas, JAMA Oncol. (2021), 7840007.

Abbreviations

AUC: Area Under the Curve
CGGA: Chinese Glioma Genome Atlas
C-index: Concordance index
CNV: Copy Number Variation
DEGs: Differentially Expressed Genes
DRGs: Disulfidptosis-Related Genes
GBM: Glioblastoma
GO: Gene Ontology
HPA: Human Protein Atlas
HR: Hazard Ratio
IDH: Isocitrate Dehydrogenase
IHC: Immunohistochemistry
KM: Kaplan-Meier
KEGG: Kyoto Encyclopedia of Genes and Genomes
LASSO: Least Absolute Shrinkage and Selection Operator
LGG: Lower-Grade Glioma
MGMT: O-6-methylguanine-DNA Methyltransferase
OS: Overall Survival
PCA: Principal Component Analysis
ROC:: Receiver Operating Characteristic
scRNA-seq: Single-Sell RNA Sequence
ssGSEA: single-sample Gene Set Enrichment Analysis
TCGA: The Cancer Genome Atlas
TIME: Tumor Immune Microenvironment
TISCH: Tumor Immune Single Cell Hub
TMB: Tumor Mutation Burden
WHO: World Health Organization